

QCD Baryons in the $1/N_c$ Expansion

Elizabeth Jenkins

*Department of Physics, 9500 Gilman Drive, University of California at San Diego, La Jolla, CA
92093-0319*

Abstract. The $1/N_c$ expansion provides a theoretical method for analyzing the spin-flavor symmetry properties of baryons in QCD that is quantitative, systematic and predictive. An exact spin-flavor symmetry exists for large- N_c baryons, whereas for QCD baryons, the spin-flavor symmetry is approximate and is broken by corrections proportional to the symmetry-breaking parameter $1/N_c = 1/3$. The $1/N_c$ expansion predicts a hierarchy of spin and flavor symmetry relations for QCD baryons that is observed in nature. It provides a quantitative understanding of why some $SU(3)$ flavor symmetry relations in the baryon sector, such as the Gell-Mann–Okubo mass formula, are satisfied to a greater precision than expected from flavor symmetry-breaking suppression factors alone.

INTRODUCTION

It has been rigorously proven that spin-flavor symmetry is an approximate symmetry of baryons in QCD [1, 2]. Spin-flavor symmetry for baryons is formally an exact symmetry in the t’Hooft large- N_c limit [3]. For finite N_c , the spin-flavor symmetry of baryons is only approximate and is broken explicitly by corrections suppressed by powers of $1/N_c$. The breaking of the large- N_c baryon spin-flavor symmetry for QCD baryons is order $1/N_c = 1/3$, which is comparable to the order 30% breaking of Gell-Mann $SU(3)$ flavor symmetry. Thus, spin-flavor symmetry is as good an approximate symmetry for QCD baryons as $SU(3)$ flavor symmetry.

Spin-flavor symmetry for QCD baryons has a long history; like $SU(3)$ flavor symmetry, spin-flavor symmetry predates the formulation of QCD. Although spin-flavor symmetry was phenomenologically successful early on [4], the physical basis for spin-flavor symmetry was not understood, even after the microscopic theory of the strong interactions was known. What has been possible in recent years is to justify spin-flavor symmetry as a *bona fide* symmetry of baryons in QCD, and to classify the explicit breakings of baryon spin-flavor symmetry to all orders in the $1/N_c$ expansion in a systematic and quantitative manner. It has been shown that the quark-gluon dynamics of large- N_c QCD gives rise to a spin-flavor symmetry for baryons. For finite N_c , the symmetry is only approximate; there are subleading $1/N_c$ corrections which explicitly break the symmetry. This new insight has led to the formulation of the baryon $1/N_c$ expansion as an expansion in operators with definite transformation properties under baryon spin and flavor symmetry. Each baryon operator in the $1/N_c$ expansion occurs at a known order in $1/N_c$. Each operator is multiplied by an unknown coefficient which is a reduced matrix element that is not determined by baryon spin-flavor symmetry. Calculating these reduced baryon matrix elements is tantamount to solving QCD in the baryon sector.

All of the new results obtained for baryons in the $1/N_c$ expansion can be characterized as symmetry relations involving spin and flavor. The spin-flavor structure of the baryon $1/N_c$ expansion yields model-independent results which are valid for QCD. It has been known for some time that the spin-flavor group theory for baryons in large- N_c QCD and in the large- N_c quark and Skyrme models is the same[5]. It is now known that a stronger statement applies: the spin-flavor structure of the baryon $1/N_c$ expansion is the same in QCD as in the quark model and the Skyrme model at each order in the $1/N_c$ expansion. In other words, the spin-flavor structure of the baryon $1/N_c$ expansion is the same in QCD as in the quark model and Skyrme models. QCD and these models, however, will differ in their predictions for the reduced matrix elements of the baryon $1/N_c$ expansion. It is well known that the quark and Skyrme models are not very successful at predicting these reduced matrix elements, which leads to the conclusion that most, if not all, of the successful predictions of the non-relativistic quark and Skyrme models are actually model-independent group-theoretic predictions, and therefore should not be regarded as evidence for the validity of these models *per se*.

The spin-flavor operator analysis of the baryon $1/N_c$ expansion has resulted in significant progress in understanding of the spin-flavor structure of baryons. It explains the extraordinary accuracy of many venerable spin-flavor and flavor symmetry relations for baryons as being due to the presence of $1/N_c$ suppression factors in addition to the usual flavor symmetry breaking suppression factors. It is remarkable that, after three decades, a quantitative understanding of spin-flavor symmetry for baryons has been achieved.

The outline of these lectures is as follows. First, a brief summary is given of the $1/N_c$ expansion of large- N_c QCD. The $1/N_c$ power counting of the quark-gluon dynamics of large- N_c QCD is described for the confined quark-gluon bound states: mesons and baryons. Second, it is shown that large- N_c baryons satisfy a contracted spin-flavor symmetry in the $N_c \rightarrow \infty$ limit. Baryon states transform as irreducible representations of the spin-flavor algebra, and operators acting on a baryon spin-flavor multiplet transform as irreducible tensor operators of the algebra.

The formalism of the baryon $1/N_c$ expansion is presented in the next section. Tensor operators acting on a baryon spin-flavor multiplet have an expansion in terms of operator products of the baryon spin-flavor generators. The order in $1/N_c$ of each operator product in the $1/N_c$ expansion is known. Not all operator products of the baryon spin-flavor generators are linearly independent, so it is necessary to eliminate redundant operator products using operator identities. This operator reduction is possible in terms of the operator identities for 2-body operator products. The complete set of 2-body operator product identities for $SU(6)$ spin-flavor symmetry is given, and then used to construct operator bases for the baryon $1/N_c$ expansion.

$1/N_c$ operator-product expansions are constructed for a number of baryon tensor operators in the final section. It is necessary to incorporate $SU(3)$ flavor symmetry breaking into the baryon $1/N_c$ expansion since $SU(3)$ breaking is comparable to the expansion parameter $1/N_c$. The $1/N_c$ expansions for baryon masses, axial vector couplings and magnetic moments are presented in detail. A comparison of experimental data with the predictions of the combined $1/N_c$ and flavor-symmetry breaking expansion is given in these cases. The presence of $1/N_c$ suppression factors in the experimental data is clearly evident, and provides a quantitative understanding of the accuracy of famous symmetry relations, such as the Gell-Mann–Okubo formula, Gell-Mann’s Equal Spacing Rule and

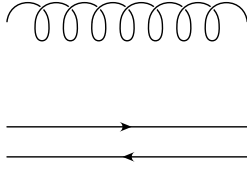


FIGURE 1. Double line notation for a gluon.

the Coleman-Glashow relation for baryon masses, as well as many others.

The focus of these lectures is on the application of the $1/N_c$ expansion to QCD baryons. The discussion is meant to be complementary to my review of large- N_c baryons [6], which is more comprehensive. The emphasis here is on baryons in QCD with $N_F = 3$ flavors of light quarks. I will try to keep the formalism introduced to a minimum throughout, although a fair amount is essential and cannot be avoided. Of necessity, a number of important topics have not been covered, even briefly. These topics include nonet symmetry of baryon amplitudes [29], exact cancellations in baryon chiral perturbation theory [44], spin-flavor symmetry of excited baryons [15], and spin-flavor symmetry of heavy quark baryons [31]. An extensive list of publications on the spin and flavor properties of baryons in the $1/N_c$ expansion is given in the references.

LARGE- N_c QCD

A recent review of large- N_c QCD can be found in Ref. [7], so the presentation here will be brief.

Large- N_c QCD is defined as the generalization of $SU(3)$ gauge theory of quarks and gluons to $SU(N_c)$ gauge theory. The naive generalization of the QCD Lagrangian is given by

$$\mathcal{L} = -\frac{1}{2} \text{Tr} G^{\mu\nu} G_{\mu\nu} + \sum_{f=1}^{N_F} \bar{q}_f (i \not{D} - m_f) q_f, \quad (1)$$

where the gauge field strength and the covariant derivative, $D^\mu = \partial^\mu + igA^\mu$, are defined as in QCD. For $SU(N_c)$ gauge theory, the gluons appear in the adjoint representation of $SU(N_c)$ with dimension $(N_c^2 - 1)$ while the quarks appear in the fundamental representation \mathbf{N}_c . Thus, there are $O(N_c)$ more gluon degrees of freedom than quark degrees of freedom in large- N_c QCD.

The $1/N_c$ power counting of quark-gluon diagrams is readily obtained by introducing t'Hooft double line notation for the gluon gauge field: the adjoint index A on the gauge field $(A^\mu)^A$ is replaced by fundamental and anti-fundamental indices i and j , so that the gauge field is written as $(A^\mu)^i_j$, a substitution which is valid up to corrections which are subleading in the $1/N_c$ expansion. In double line notation, the gluon is effectively replaced by a quark line and an antiquark line, as shown in Fig. 1. When a quark-gluon Feynman diagram is rewritten in double line notation, determining the power in N_c of the diagram is equivalent to counting the number of closed quark loops with unrestricted color summations. Fig. 2 gives an explicit example of this $1/N_c$

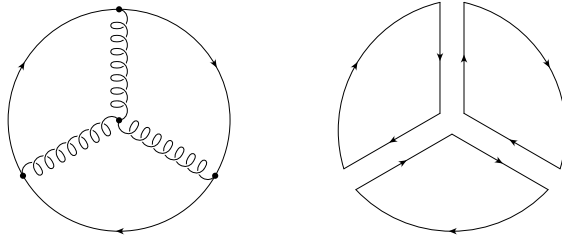


FIGURE 2.

counting. The diagram shown in Fig. 2 reduces to three quark loops, and is therefore proportional to N_c^3 . In addition, the diagram is proportional to four powers of the quark-gluon coupling constant g , since the diagram contains four vertices, each of which is proportional to g . Thus, the overall diagram is proportional to $g^4 N_c^3 = (g^2 N_c)^2 N_c$. A simple analysis of other diagrams leads to the t'Hooft result that vacuum Feynman diagrams are proportional to

$$(g^2 N_c)^{\frac{1}{2}V_3+V_4} N_c^\chi, \quad (2)$$

where V_n is the number of n -point vertices in the diagram and χ is the Euler character of the diagram. Consequently, diagrams with arbitrary numbers of 3- and 4-point vertices grow with arbitrarily large powers of N_c unless the limit $N_c \rightarrow \infty$ is taken with $g^2 N_c$ held fixed. This limiting procedure, which is necessary to define $SU(N_c)$ gauge theory in the large- N_c limit, is known as the t'Hooft limit. The constraint $g^2 N_c$ held fixed can be implemented by rescaling the gauge coupling $g \rightarrow g/\sqrt{N_c}$ in the original Lagrangian. After this rescaling, Feynman diagrams will be proportional to N_c^χ , where the Euler character $\chi = 2 - 2H - L$ can be computed in terms of the number of handles H and quark loops L of a given diagram. The t'Hooft limit leads to the following results:

- For finite and large N_c , planar diagrams with $H = 0$ dominate the dynamics. (All planar diagrams with a given L are of the same order.)
- Diagrams with nonplanar gluon exchange ($H \neq 0$) are suppressed relative to planar diagrams by one factor of $1/N_c^2$ for each nonplanar gluon.
- Diagrams with quark loops ($L \neq 0$) are suppressed by one factor of $1/N_c$ for each quark loop.

The dynamics of large- N_c QCD is presumed to be confining. The β function of large- N_c QCD implies that the rescaled coupling gets large at some scale, let us call it Λ_{QCD} . For $E \leq O(\Lambda_{\text{QCD}})$, large- N_c QCD is strongly coupled and is expected to exhibit confinement. The confined theory contains colorless bound states: mesons, baryons and glueballs. The $1/N_c$ power counting for large- N_c mesons and for baryons is summarized below.

A meson in large- N_c QCD is created with unit amplitude by the operator

$$\frac{1}{\sqrt{N_c}} \sum_{i=1}^{N_c} \bar{q}_i q^i, \quad (3)$$

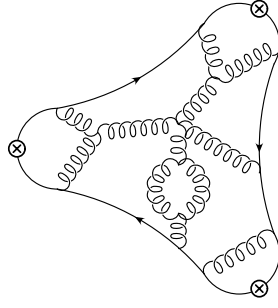


FIGURE 3. A planar diagram contributing to a meson three-point vertex at leading order.

where i is the color index of the quark. The N_c -dependence of meson amplitudes can be obtained by studying quark-gluon diagrams. The leading diagrams are planar diagrams with a single quark loop ($L = 1$) with all insertions of meson operators on the quark loop. An 3-meson diagram is shown in Fig. 3 as an example. The leading diagrams for an n -meson amplitude are $O(N_c^{1-n/2})$. For example, a meson decay constant is $O(\sqrt{N_c})$; a meson mass is $O(1)$; a 3-meson coupling is $O(1/\sqrt{N_c})$, and so forth. This power counting implies that large- N_c mesons are narrow states which are weakly coupled to one another [8, 9].

The situation for baryons is qualitatively different. A large- N_c baryon is a bound state of N_c valence quarks completely antisymmetrized in the color indices of the quarks,

$$\varepsilon_{i_1 i_2 i_3 \dots i_{N_c}} q^{i_1} q^{i_2} q^{i_3} \dots q^{i_{N_c}} . \quad (4)$$

The mass of the baryon is $O(N_c)$, whereas the size of the baryon is $O(1)$. The N_c -dependence of baryon-meson scattering amplitudes and couplings can be determined by studying the N_c -counting of quark-gluon diagrams. An antibaryon-baryon- n -meson vertex is $O(N_c^{1-n/2})$, as is an amplitude for the scattering baryon+meson \rightarrow baryon + $(n - 1)$ mesons.

Naively, this power counting is inconsistent. The amplitude for baryon + meson \rightarrow baryon + meson scattering is $O(1)$, whereas an antibaryon-baryon-meson vertex is $O(\sqrt{N_c})$, and grows with N_c . A tree diagram with two different single-meson-baryon vertices produces an amplitude which is $O(N_c)$, not $O(1)$. Unless the $O(N_c)$ contributions of different tree diagrams all cancel one another exactly, the total scattering amplitude is $O(N_c)$ and will violate the $1/N_c$ power counting. Imposing the constraint that the scattering amplitude be $O(1)$ results in relations amongst single-meson-baryon-antibaryon vertices which must be satisfied for consistency of the $1/N_c$ power counting for baryon-meson scattering amplitudes. Consistency of $1/N_c$ power counting for baryon-meson scattering amplitudes and vertices results in non-trivial constraints on large- N_c baryon matrix elements at leading and subleading orders [1, 2]. Large- N_c consistency conditions also lead to the derivation of contracted spin-flavor symmetry for baryons [1, 10].

SPIN-FLAVOR SYMMETRY OF LARGE- N_C BARYONS

Large- N_c contracted spin-flavor symmetry can be derived by considering pion-baryon scattering at low energies $E \sim O(1)$. In this kinematic regime, the large- N_c baryon acts as a heavy static source for scattering the pion with no recoil. There are two tree diagrams which contribute to the scattering amplitude at $O(N_c)$, the direct and crossed diagrams. Using the N_c -independent baryon propagator of Heavy Baryon Chiral Perturbation Theory [11], it is easy to show that cancellation of the $O(N_c)$ scattering amplitude from these two diagrams is given by the large- N_c consistency condition [1]

$$N_c [X^{ia}, X^{jb}] \leq O(1), \quad (5)$$

where the baryon axial vector couplings (in the baryon rest frame) are defined by

$$A^{ia} \equiv g N_c X^{ia}. \quad (6)$$

Expanding the operator X^{ia} in a power series in $1/N_c$,

$$X^{ia} = X_0^{ia} + \frac{1}{N_c} X_1^{ia} + \frac{1}{N_c^2} X_2^{ia} + \dots, \quad (7)$$

and substituting into Eq. (5) yields the constraint

$$[X_0^{ia}, X_0^{jb}] = 0 \quad (8)$$

for the leading $O(N_c)$ matrix elements of the baryon axial vector couplings. As we will see, the matrix elements of X_0^{ia} between different baryon states are all determined relative to one another by this constraint, so the $O(N_c)$ portion of the baryon axial vector couplings A^{ia} are all related by symmetry up to an overall normalization constant given by the coupling g , which is the reduced matrix element of the axial vector couplings.

The operator X_0^{ia} is an irreducible tensor operator transforming according to the spin-1, $SU(3)$ adjoint representation of spin \otimes flavor, so the commutators of X_0^{ia} with the baryon spin and flavor generators are given by

$$[J^i, X_0^{ja}] = i\epsilon^{ijk} X_0^{ka}, \quad [T^a, X_0^{ib}] = if^{abc} X_0^{ic}. \quad (9)$$

The Lie algebra of the baryon spin \otimes flavor generators, together with Eqs. (8) and (9), yields a contracted spin-flavor algebra [1, 10]

$$\begin{aligned} [J^i, J^j] &= i\epsilon^{ijk} J^k, & [T^a, T^b] &= if^{abc} T^c, & [J^i, T^a] &= 0, \\ [J^i, X_0^{ja}] &= i\epsilon^{ijk} X_0^{ka}, & [T^a, X_0^{ib}] &= if^{abc} X_0^{ic} \\ [X_0^{ia}, X_0^{jb}] &= 0 \end{aligned} \quad (10)$$

in the large- N_c limit.

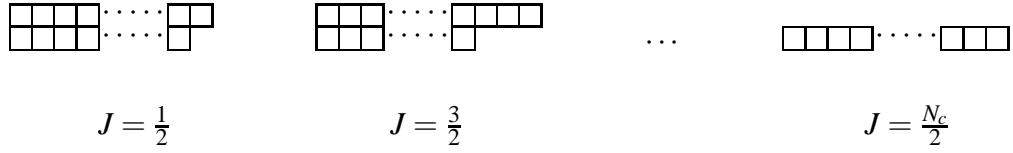


FIGURE 4. Decomposition of the $SU(6)$ baryon representation $\square\square\square\square\cdots\square\square\square$ into $SU(2) \otimes SU(3)$ baryon representations. Each Young tableau has N_c boxes.

It is instructive to contrast the contracted spin-flavor algebra with the $SU(6)$ spin-flavor algebra

$$\begin{aligned}
 [J^i, J^j] &= i\varepsilon^{ijk} J^k, & [T^a, T^b] &= if^{abc} T^c, & [J^i, T^a] &= 0, \\
 [J^i, G^{ja}] &= i\varepsilon^{ijk} G^{ka}, & [T^a, G^{ib}] &= if^{abc} G^{ic}, & & \\
 [G^{ia}, G^{jb}] &= \frac{i}{6} \delta^{ab} \varepsilon^{ijk} J^k + \frac{i}{4} \delta^{ij} f^{abc} T^c + \frac{i}{2} \varepsilon^{ijk} d^{abc} G^{kc}. & & & &
 \end{aligned} \tag{11}$$

The contracted spin-flavor algebra can be obtained from the $SU(6)$ spin-flavor algebra with the identification

$$\lim_{N_c \rightarrow \infty} \frac{G^{ia}}{N_c} \rightarrow X_0^{ia}. \tag{12}$$

Thus, the $SU(6)$ spin-flavor algebra correctly reproduces the contracted spin-flavor algebra in the large- N_c limit. It differs from the contracted spin-flavor algebra by the inclusion of some subleading $1/N_c$ terms in the generators G^{ia} .

The contracted spin-flavor algebra in the large- N_c limit leads to baryon spin-flavor representations which are infinite-dimensional. For finite N_c , it is convenient to work with the $SU(6)$ spin-flavor algebra which leads to finite-dimensional baryon representations. Since the emphasis of these lectures is on QCD baryons with $N_c = 3$, the spin-flavor symmetry will be implemented for finite N_c . Discussion of the connection between finite-dimensional and infinite-dimensional baryon representations can be found in Ref. [6].

The lowest-lying large- N_c baryon representation of the spin-flavor algebra is given by the completely symmetric tensor product of N_c quarks in the fundamental rep of spin-flavor. Under the breakdown of spin-flavor symmetry to its spin \otimes flavor subgroup, the completely symmetric spin-flavor representation decomposes into the spin and flavor representations displayed in Fig. 4. The baryon spin-flavor representation contains baryons with spins $J = \frac{1}{2}, \frac{3}{2}, \frac{5}{2}, \dots, \frac{N_c}{2}$. The $SU(3)$ flavor representation of the baryons with a given spin J is given by the same Young tableau as its spin $SU(2)$ representation. The dimensions of the spin representations do not vary with N_c , but the dimensions of the flavor representations do. Consequently, the $SU(3)$ flavor multiplets are considerably more complicated for $N_c > 3$ than they are in QCD. The (T^3, T^8) weight diagrams for the spin-1/2 and spin-3/2 flavor multiplets for large- N_c baryons are given in Figs. 5 and 6. The numbers appearing in the weight diagrams denote the degeneracy of each weight. While there are many additional baryon states for $N_c > 3$, for $N_c = 3$ these flavor representations reduce to the usual octet and decuplet multiplets, respectively. In the

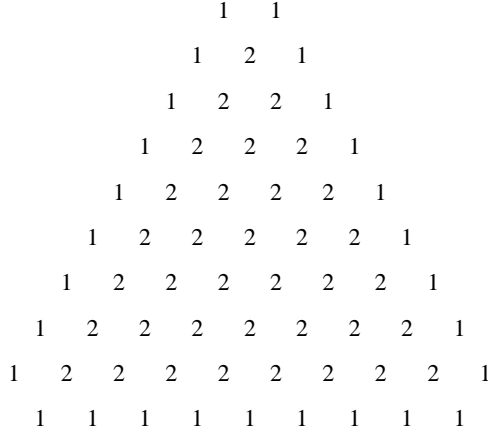


FIGURE 5. $SU(3)$ weight diagram of spin- $\frac{1}{2}$ baryons for large N_c .

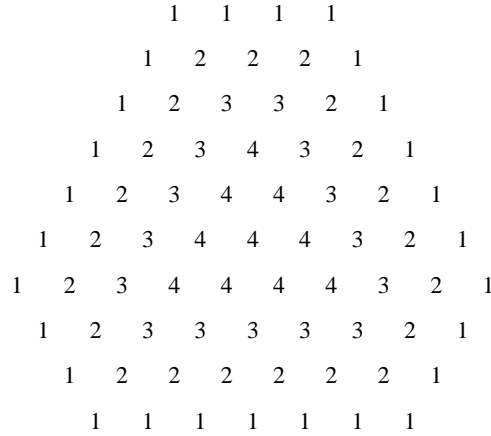


FIGURE 6. $SU(3)$ weight diagram of the spin- $\frac{3}{2}$ baryons for large N_c .

end, we will apply the $1/N_c$ expansion to QCD baryons with $N_c = 3$, and there will be no unphysical baryon states in the expansion.

$1/N_c$ EXPANSION FOR BARYONS

The $1/N_c$ expansion of any baryon operator can be obtained by solving large- N_c consistency conditions. Each baryon operator has a $1/N_c$ expansion in terms of all independent operator products which can be constructed from the baryon spin-flavor generators.

The general form of the baryon $1/N_c$ expansion is given by

$$O_{\text{QCD}}^m = N_c^m \sum_{n=0}^{N_c} c_n \frac{1}{N_c^n} O^n, \quad (13)$$

where O_{QCD}^m is an m -body quark operator in QCD which acts on baryon states. The baryon matrix elements of an m -body QCD quark operator can be at most $O(N_c^m)$,

which is reflected in the factor of N_c^m in front of the $1/N_c$ operator expansion. The $1/N_c$ expansion sums over all independent operators which transform according to the same representation of spin \otimes flavor symmetry as the QCD operator. The independent operators O^n which form a basis for the $1/N_c$ expansion are n^{th} degree polynomials of the baryon spin-flavor generators J^i , T^a and G^{ia} . The baryon matrix elements of these operator products can be computed in terms of the matrix elements of the baryon spin-flavor generators. The order in $1/N_c$ at which each independent operator product appears in the $1/N_c$ expansion also is known. $1/N_c$ power counting implies that an n -body operator product is multiplied by an explicit factor of $1/N_c^n$, or that each spin-flavor generator in an operator product is accompanied by a factor of $1/N_c$. Since the matrix elements of an n -body operator product are $\leq O(N_c^n)$, the matrix elements of each term in the $1/N_c$ operator expansion are manifestly $\leq O(N_c^m)$, as required. Every operator in the operator basis is accompanied by an unknown coefficient c_n , which is a reduced matrix element of the spin-flavor $1/N_c$ expansion and is not predicted by spin-flavor symmetry. The coefficients are $O(1)$ at leading order in the $1/N_c$ expansion. Finally, the summation over spin-flavor operators O^n only extends to N_c -body quark operators, since all n -body quark operators with $n > N_c$ will be redundant operators on baryons composed of N_c valence quarks.

Each operator O^n in the operator basis of the $1/N_c$ expansion can be written as an n -body quark operator using bosonic quarks which carry only spin and flavor quantum numbers. Let q^α represent an annihilation operator for a bosonic quark with spin-flavor $\alpha = 1, \dots, 6$, and let q_α^\dagger represent the corresponding creation operator. In terms of these creation/annihilation operators, all n -body quark operators acting on baryon states can be catalogued. There is only a single 0-body quark operator, the baryon identity operator $\mathbb{1}$, which does not act on any of the valence quarks in the baryon. The 1-body quark operators are given by $q^\dagger q$ and the baryon spin-flavor generators

$$\begin{aligned} J^i &= q^\dagger \left(\frac{\boldsymbol{\sigma}^i}{2} \otimes \mathbb{1} \right) q, \\ T^a &= q^\dagger \left(\mathbb{1} \otimes \frac{\lambda^a}{2} \right) q, \\ G^{ia} &= q^\dagger \left(\frac{\boldsymbol{\sigma}^i}{2} \otimes \frac{\lambda^a}{2} \right) q. \end{aligned} \tag{14}$$

The notation here is compact. Each 1-body quark operator is understood to act on each quark line in the baryon. Thus,

$$G^{ia} = \sum_\ell q_\ell^\dagger \left(\frac{\boldsymbol{\sigma}^i}{2} \otimes \frac{\lambda^a}{2} \right) q_\ell. \tag{15}$$

In addition, note that $q^\dagger q = N_c \mathbb{1}$ is not an independent operator and can be eliminated from the list of 1-body quark operators. The 2-body quark operators are given by products of the 1-body quark operators, the baryon spin-flavor generators. Each 2-body operator product can be written as the symmetric product (or anticommutator) of two 1-body operators since the commutator of any two 1-body operators can be replaced by

TABLE 1. $SU(6)$ Operator Identities

Identity	(J , SU(3))
$2 \{J^i, J^i\} + 3 \{T^a, T^a\} + 12 \{G^{ia}, G^{ia}\} = 5N_c(N_c + 6)$	(0, 0)
$d^{abc} \{G^{ia}, G^{ib}\} + \frac{2}{3} \{J^i, G^{ic}\} + \frac{1}{4} d^{abc} \{T^a, T^b\} = \frac{2}{3} (N_c + 3) T^c$	(0, 8)
$\{T^a, G^{ia}\} = \frac{2}{3} (N_c + 3) J^i$	(1, 0)
$\frac{1}{3} \{J^k, T^c\} + d^{abc} \{T^a, G^{kb}\} - \epsilon^{ijk} f^{abc} \{G^{ia}, G^{jb}\} = \frac{4}{3} (N_c + 3) G^{kc}$	(1, 8)
$-12 \{G^{ia}, G^{ia}\} + 27 \{T^a, T^a\} - 32 \{J^i, J^i\} = 0$	(0, 0)
$d^{abc} \{G^{ia}, G^{ib}\} + \frac{9}{4} d^{abc} \{T^a, T^b\} - \frac{10}{3} \{J^i, G^{ic}\} = 0$	(0, 8)
$4 \{G^{ia}, G^{ib}\} = \{T^a, T^b\} \quad (27)$	(0, 27)
$\epsilon^{ijk} \{J^i, G^{jc}\} = f^{abc} \{T^a, G^{kb}\}$	(1, 8)
$3 d^{abc} \{T^a, G^{kb}\} = \{J^k, T^c\} - \epsilon^{ijk} f^{abc} \{G^{ia}, G^{jb}\}$	(1, 8)
$\epsilon^{ijk} \{G^{ia}, G^{jb}\} = f^{acg} d^{bch} \{T^g, G^{kh}\} \quad (10 + \overline{10})$	(1, 10 + $\overline{10}$)
$3 \{G^{ia}, G^{ja}\} = \{J^i, J^j\} \quad (J = 2)$	(2, 0)
$3 d^{abc} \{G^{ia}, G^{jb}\} = \{J^i, G^{jc}\} \quad (J = 2)$	(2, 8)

a linear combination of 1-body operators by the spin-flavor algebra. This observation also applies to all n -body operators with $n \geq 2$.

Not all operator products of the spin-flavor generators are linearly dependent, so it is necessary to eliminate redundant operators using operator identities. The complete set of 2-body operator identities for the completely symmetric baryon representation of $SU(6)$ are given in Table 1 along with their respective spin \otimes flavor representations [25]. It is possible to eliminate all redundant n -body operators by using the 2-body operator identities, so Table 1 gives the complete set of operator identities.

The group theory behind Table 1 is interesting. Purely n -body quark operators are normal-ordered operators of the form

$$q_{\alpha_1}^\dagger \cdots q_{\alpha_n}^\dagger T_{\beta_1 \cdots \beta_n}^{\alpha_1 \cdots \alpha_n} q^{\beta_1} \cdots q^{\beta_n}. \quad (16)$$

For the completely symmetric $SU(6)$ representation of baryon states, the only nonvanishing normal-ordered quarks operators have tensors T which are totally symmetric in the upper and the lower spin-flavor indices. We would like to reexpress these independent normal-ordered operators as operator products of the spin-flavor generators, whose baryon matrix elements are known.

The group theory behind the operator identities is particularly elegant. The 0-body quark operator $\mathbb{1}$ is in the singlet representation of $SU(6)$, whereas the 1-body operators transform as the tensor product of a fundamental and antifundamental of $SU(6)$, which decomposes into a singlet and an adjoint of $SU(6)$. The 2-body operators are obtained from the tensor product of the symmetric 2-quark representation and its conjugate. Specifically,

$$\begin{aligned} 0\text{-body} &: 1 \\ 1\text{-body} &: \left(\overline{\square} \otimes \square \right) = 1 + \text{adj} = 1 + T_\beta^\alpha \end{aligned} \quad (17)$$

$$2\text{-body} : \left(\overline{\square\square} \otimes \square\square \right) = 1 + T_{\beta}^{\alpha} + T_{(\beta_1\beta_2)}^{(\alpha_1\alpha_2)}.$$

There are identities which relate the singlet and adjoint 2-body operators to 1-body adjoint and 0-body singlet operators, so the 2-body operators which transform as the singlet and the adjoint are not independent. The relevant identities are most easily understood keeping $SU(6)$ symmetry manifest. The generators J^i , T^a and G^{ia} form a complete set of $SU(6)$ generators Λ^A , $A = 1, \dots, 35$. The operator identities relating the singlet 2-body operators to the 0-body operator and the adjoint 2-body operators to the 1-body operators are given by the Casimir identities

$$\begin{aligned} \Lambda^A \Lambda^A &= C(R) \mathbb{1} \\ d^{ABC} \Lambda^B \Lambda^C &= D(R) \Lambda^A, \end{aligned} \quad (18)$$

where $C(R)$ and $D(R)$ are the quadratic and cubic Casimirs for the $SU(6)$ baryon representation R . These Casimir identities for the completely symmetric baryon spin-flavor representation produce the operator identities in the first two blocks of Table 1. The remaining 2-body operator identities arise because the completely symmetric product of two $SU(6)$ adjoints,

$$(\text{adj} \otimes \text{adj})_S = 1 + T_{\beta}^{\alpha} + T_{[\beta_1\beta_2]}^{[\alpha_1\alpha_2]} + T_{(\beta_1\beta_2)}^{(\alpha_1\alpha_2)}, \quad (19)$$

contains an additional tensor structure. The 2-body operator products corresponding to the tensor $T_{[\beta_1\beta_2]}^{[\alpha_1\alpha_2]}$ will vanish identically when acting on the completely symmetric baryon spin-flavor representation. These operator product combinations yield the vanishing operator identities given in the third part of Table 1.

The above operator identities are summarized by the following operator reduction rule: All operators in which two flavor indices are contracted using δ^{ab} , d^{abc} , or f^{abc} or two spin indices on G 's are contracted using δ^{ij} or ϵ^{ijk} can be eliminated.

QCD BARYONS

I will now derive $1/N_c$ expansions for the masses, axial vector currents and magnetic moments of baryons in QCD. $SU(3)$ flavor breaking cannot be neglected relative to $1/N_c$, and is included in the analysis. For large- N_c baryons, the $1/N_c$ expansion extends up to N_c -body operators, so the $1/N_c$ expansion for QCD baryons goes up to third order in the generators. The $1/N_c$ expansion including flavor symmetry breaking also goes up to N_c -body operators, so perturbative $SU(3)$ breaking extends to finite order in flavor symmetry breaking. For a baryon operator with a $1/N_c$ expansion beginning with a n -body operator, the flavor symmetry breaking expansion extends to order $(N_c - n)$.

Masses

The baryon mass operator is a $J = 0$ operator. The leading operator in the $1/N_c$ expansion is the flavor singlet operator $N_c \mathbb{1}$ which gives the same $O(N_c)$ mass to all baryons

in a spin-flavor representation. Since the $1/N_c$ expansion begins with a 0-body operator, the baryon mass operator can be expanded to third order in flavor symmetry breaking. Thus, the baryon mass operator decomposes into the $SU(3)$ flavor representations

$$M = M^{\mathbf{1}} + M^{\mathbf{8}} + M^{\mathbf{27}} + M^{\mathbf{64}}, \quad (20)$$

where the singlet, octet, **27** and **64** are zeroth, first, second and third order in $SU(3)$ flavor symmetry breaking, respectively. Each of these spin-singlet flavor representations has a $1/N_c$ operator expansion. The $1/N_c$ expansions are given by

$$\begin{aligned} M^{\mathbf{1}} &= N_c \mathbf{1} + \frac{1}{N_c} J^2, \\ M^{\mathbf{8}} &= T^8 + \frac{1}{N_c} \{J^i, G^{i8}\} + \frac{1}{N_c^2} \{J^2, T^8\}, \\ M^{\mathbf{27}} &= \frac{1}{N_c} \{T^8, T^8\} + \frac{1}{N_c^2} \{T^8, \{J^i, G^{i8}\}\}, \\ M^{\mathbf{64}} &= \frac{1}{N_c^2} \{T^8, \{T^8, T^8\}\}, \end{aligned} \quad (21)$$

where it is to be understood that there is an unknown coefficient multiplying each operator in the above $1/N_c$ expansions. Note that the operators in these expansions can be derived using the operator identities in Table 1. For example, consider the octet mass expansion. $SU(3)$ flavor breaking transforms as the eighth component of an octet. There is only one 1-body operator which is $J = 0$ and the eighth component of an $SU(3)$ octet, namely T^8 . From Table 1, one finds that there are three 2-body operators which transform in this manner: $d^{ab8} \{G^{ia}, G^{ib}\}$, $d^{ab8} \{T^a, T^b\}$ and $\{J^i, G^{i8}\}$. However, Table 1 shows that one linear combination of these operators is proportional to the 1-body operator T^8 , and that another linear combination vanishes for the completely symmetric $SU(6)$ baryon representation. Thus, there is only one independent 2-body operator. This 2-body operator is taken to be $\{J^i, G^{i8}\}$ by the operator reduction rule. Application of the 2-body identities implies that there is a single independent 3-body operator which transforms as a spin singlet and as the eighth component of a flavor octet. Without loss of generality, this operator can be taken to be $\{J^2, T^8\}$. Similar analyses produce the other expansions in Eq. (21).

The $1/N_c$ expansion of the baryon mass operator given by Eqs. (20) and (21) contains eight independent operators, which is equal to the number of baryon masses in the **56** of $SU(6)$: the N , Λ , Σ , Ξ , Δ , Σ^* , Ξ^* , Ω . Each mass operator contributes to a unique linear combination of these eight masses. These linear combinations are given in Table 2[26]. Each mass combination occurs at specific orders in the $1/N_c$ and $SU(3)$ flavor breaking expansions; these suppression factors also appear in Table 2. The parameter $\varepsilon \sim m_s/\Lambda_{\text{QCD}}$ is the suppression factor for $SU(3)$ flavor symmetry breaking. The final column gives the experimental value for the accuracy of each mass combination, which is defined by the dimensionless quantity

$$\frac{\sum B_i}{\sum |B_i|/2} \quad (22)$$

TABLE 2. Baryon Mass Hierarchy

Mass Splitting	$1/N_c$	Flavor	Expt.
$\frac{5}{8}(2N + 3\Sigma + \Lambda + 2\Xi) - \frac{1}{10}(4\Delta + 3\Sigma^* + 2\Xi^* + \Omega)$	N_c	1	*
$\frac{1}{8}(2N + 3\Sigma + \Lambda + 2\Xi) - \frac{1}{10}(4\Delta + 3\Sigma^* + 2\Xi^* + \Omega)$	$1/N_c$	1	$18.21 \pm 0.03\%$
$\frac{5}{2}(6N - 3\Sigma + \Lambda - 4\Xi) - (2\Delta - \Xi^* - \Omega)$	1	ε	$20.21 \pm 0.02\%$
$\frac{1}{3}(N - 3\Sigma + \Lambda + \Xi)$	$1/N_c$	ε	$5.94 \pm 0.01\%$
$\frac{1}{2}(-2N - 9\Sigma + 3\Lambda + 8\Xi) + (2\Delta - \Xi^* - \Omega)$	$1/N_c^2$	ε	$1.11 \pm 0.02\%$
$\frac{5}{4}(2N - \Sigma - 3\Lambda + 2\Xi) - \frac{1}{7}(4\Delta - 5\Sigma^* - 2\Xi^* + 3\Omega)$	$1/N_c$	ε^2	$0.37 \pm 0.01\%$
$\frac{1}{2}(2N - \Sigma - 3\Lambda + 2\Xi) - \frac{1}{7}(4\Delta - 5\Sigma^* - 2\Xi^* + 3\Omega)$	$1/N_c^2$	ε^2	$0.17 \pm 0.02\%$
$\frac{1}{4}(\Delta - 3\Sigma^* + 3\Xi^* - \Omega)$	$1/N_c^2$	ε^3	$0.09 \pm 0.03\%$

computed for each mass combination.

The $1/N_c$ and flavor symmetry breaking hierarchy predicted for the baryon masses can be tested by comparing the experimental accuracies to the $1/N_c$ and ε suppression factors. The numerical accuracies of the mass combinations are plotted in Fig. 7, except for the mass combination corresponding to the $N_c\mathbf{1}$ operator. The hierarchy predicted by the $1/N_c$ suppression factors is clearly evident. For example, there are three mass combinations that are first order in $SU(3)$ breaking, but of order $1/N_c$, $1/N_c^2$ and $1/N_c^3$ relative to the leading $O(N_c)$ singlet mass of the baryons. This pattern can be seen in Fig. 7. In addition, the two flavor-**27** mass combinations which are second order in $SU(3)$ breaking are suppressed by factors of $1/N_c^2$ and $1/N_c^3$ relative to the leading $O(N_c)$ baryon mass. The Gell-Mann–Okubo flavor-**27** mass splitting of the spin-1/2 baryon octet,

$$\frac{1}{4}(2N - \Sigma - 3\Lambda + 2\Xi), \quad (23)$$

and the flavor-**27** Equal Spacing Rule mass splitting of the spin-3/2 baryon decuplet,

$$\frac{1}{7}(4\Delta - 5\Sigma^* - 2\Xi^* + 3\Omega), \quad (24)$$

are linear combinations of the two flavor-**27** mass splittings specified by the $1/N_c$ expansion, so each is predicted to be a factor of $1/N_c^2$ more accurate than expected from flavor symmetry breaking factors alone. The most suppressed mass splitting is the flavor-**64** Equal Spacing Rule mass splitting,

$$\frac{1}{4}(\Delta - 3\Sigma^* + 3\Xi^* - \Omega), \quad (25)$$

which is third order in $SU(3)$ flavor breaking and of relative order $1/N_c^3$. This mass combination is clearly suppressed by a greater factor than predicted from $SU(3)$ breaking alone. The experimental accuracy of this mass combination is consistent with the $1/N_c$ hierarchy, but a better measurement of the splitting is needed to test the $1/N_c^3$ prediction of the $1/N_c$ expansion definitively.

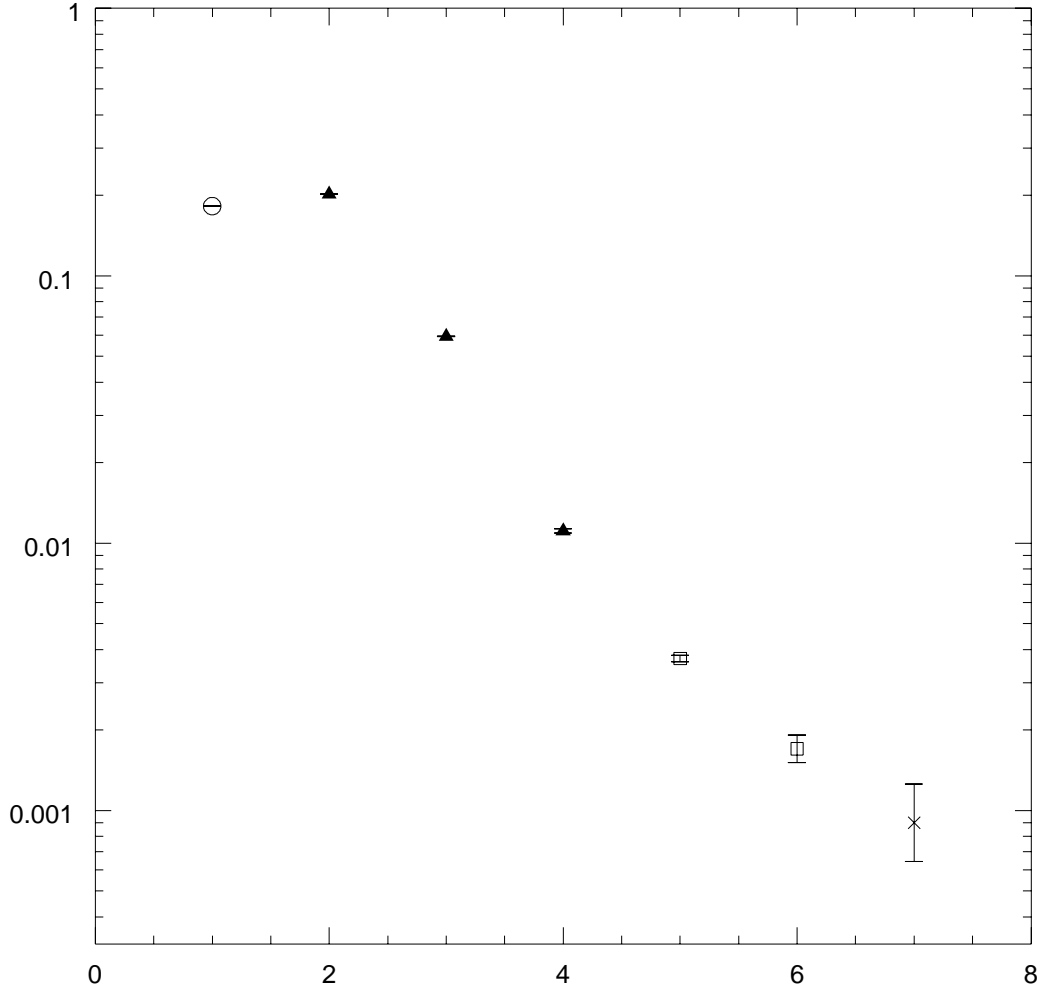


FIGURE 7. Baryon mass hierarchy. The mass combinations are of relative order $\frac{1}{N_c^2}, \frac{\epsilon}{N_c}, \frac{\epsilon}{N_c^2}, \frac{\epsilon}{N_c^3}, \frac{\epsilon^2}{N_c^2}, \frac{\epsilon^2}{N_c^3}, \frac{\epsilon^3}{N_c^2}$ compared to the overall $O(N_c)$ singlet mass of the baryon **56**.

In summary, the $1/N_c$ hierarchy is observed in the $I = 0$ baryon mass splittings, and the presence of $1/N_c$ suppression factors explains the accuracy of baryon mass combinations quantitatively.

There also is clear evidence for the $1/N_c$ hierarchy in the $I = 1$ baryon mass splittings. For example, the Coleman-Glashow mass splitting

$$[(p - n) - (\Sigma^+ - \Sigma^-) + (\Xi^0 - \Xi^-)] \quad (26)$$

has been measured to be non-zero for the first time quite recently. The measured mass splitting is more accurate than the prediction based on flavor suppression fac-

tors alone, and is consistent with an additional $1/N_c^2$ suppression predicted by the $1/N_c$ expansion[26]. It is particularly noteworthy that this prediction of the $1/N_c$ expansion was made before the Coleman-Glashow mass splitting was measured to the precision required to test the $1/N_c$ hierarchy. A more in-depth discussion of the $I = 1$ baryon mass splittings can be found in Refs. [45] and [46].

Axial Vector Couplings

The baryon axial vector current operator A^{ia} is $J = 1$ and an $SU(3)$ flavor adjoint. In the $SU(3)$ symmetry limit, the $1/N_c$ expansion of the baryon axial vector current is given by[25]

$$A^{ia} = a_1 G^{ia} + b_2 \frac{1}{N_c} J^i T^a + b_3 \frac{1}{N_c^2} \{J^i, \{J^j, G^{ja}\}\} + d_3 \frac{1}{N_c^2} \left(\{J^2, G^{ia}\} - \frac{1}{2} \{J^i, \{J^j, G^{ja}\}\} \right), \quad (27)$$

where the $1/N_c$ expansion for QCD baryons extends up to 3-body operators. The $1/N_c$ expansion involves four independent operators, so the baryon axial vector couplings are determined in terms of the four unknown coefficients a_1 , b_2 , b_3 and d_3 . The usual $SU(3)$ flavor analysis of the axial vector couplings of the spin-1/2 baryon octet and spin-3/2 decuplet is given in terms of the four $SU(3)$ couplings D , F , C and H ,

$$2D \text{Tr } \bar{B} S^\mu \{ \mathcal{A}_\mu, B \} + 2F \text{Tr } \bar{B} S^\mu [\mathcal{A}_\mu, B] + C (\bar{T}^\mu \mathcal{A}_\mu B + \bar{B} \mathcal{A}_\mu T^\mu) + 2H \bar{T}^\mu S^\nu \mathcal{A}_\nu T_\mu, \quad (28)$$

where B represents the baryon octet, T^μ denotes the baryon decuplet, S^μ is a spin operator, and \mathcal{A}^μ is the axial vector current of the pion octet. The coefficients of the $1/N_c$ parametrization and the $SU(3)$ couplings are related by

$$\begin{aligned} D &= \frac{1}{2} a_1 + \frac{1}{6} b_3, \\ F &= \frac{1}{3} a_1 + \frac{1}{6} b_2 + \frac{1}{9} b_3, \\ C &= -a_1 - \frac{1}{2} d_3, \\ H &= -\frac{3}{2} a_1 - \frac{3}{2} b_2 - \frac{5}{2} b_3. \end{aligned} \quad (29)$$

The $1/N_c$ expansion for the baryon axial vector current can be truncated after the first two operators in Eq. (27) since the two 3-body operators are both suppressed relative to the 1-body operator by a factor of $1/N_c^2$. The 2-body operator $J^i T^a$ can not be neglected relative to the 1-body operator G^{ia} for all $a = 1, \dots, 8$, so the leading order result for A^{ia} is given by

$$A^{ia} = a_1 G^{ia} + b_2 \frac{1}{N_c} J^i T^a, \quad (30)$$

in terms of two parameters a_1 and b_2 . The operator G^{ia} alone produces axial vector couplings with $SU(6)$ symmetry. If only the G^{ia} operator is retained, the four $SU(3)$ couplings satisfy

$$F/D = 2/3, \quad C = -2D, \quad H = -3F. \quad (31)$$

The operator $J^i T^a$ breaks the $SU(6)$ symmetry. The breaking is such that the $SU(3)$ couplings are related by

$$C = -2D, \quad H = 3D - 9F, \quad (32)$$

which reduces to $SU(6)$ symmetry when $F/D = 2/3$.

It is worthwhile to consider the isospin decomposition of A^{ia} into the isovector, isodoublet and isosinglet axial vector currents. The $1/N_c$ expansion for the isovector axial vector current is given by

$$A^{ia} = a_1 G^{ia} + b_2 \frac{1}{N_c} J^i I^a, \quad a = 1, 2, 3. \quad (33)$$

The 2-body operator $J^i I^a$ is suppressed relative to G^{ia} for $a = 1, 2, 3$, since the matrix elements of G^{ia} are $O(N_c)$ whereas the matrix elements of J^i and I^a are both $O(1)$. Thus, the $1/N_c$ expansion for the isovector current can be truncated to the 1-body operator G^{i3} up to a correction of order $1/N_c^2$ relative to the leading $O(N_c)$ term. A fit to the pion couplings yields $F/D = 2/3$ up to a correction of relative order $1/N_c^2$. Similar reasoning for the isodoublet axial vector current gives $F/D = 2/3$ up to a correction of relative order $1/N_c$. The 2-body operator cannot be neglected relative to the 1-body operator G^{ia} for the isosinglet axial vector current with $a = 8$.

The $1/N_c$ operator expansion for the flavor-octet baryon axial vector current can be generalized to include $SU(3)$ breaking. The $SU(3)$ -symmetric expansion begins with a 1-body operator, so the baryon axial vector currents need to be expanded to second order in $SU(3)$ symmetry breaking. However, many of the baryon axial vector current observables are not measured, so it is not necessary to construct the $1/N_c$ expansion to all orders in $SU(3)$ breaking. Instead, the $1/N_c$ expansion will be considered to linear order in $SU(3)$ breaking.

The expansion at linear order in $SU(3)$ breaking involves additional spin-1 operators in different flavor representations,

$$\delta A^{ia} = A_{\mathbf{1}}^{ia} + A_{\mathbf{8}_S}^{ia} + A_{\mathbf{8}_A}^{ia} + A_{\mathbf{27}}^{ia} + A_{\mathbf{10}+\mathbf{10}}^{ia}. \quad (34)$$

A valid truncation of the $1/N_c$ expansion to first order in $SU(3)$ breaking was constructed in Ref. [25]. The $1/N_c$ expansion is given by

$$\begin{aligned} A^{ia} &= \left(a_1 \delta^{ab} + c_1 d^{ab8} \right) G^{ib} + \left(b_2 \delta^{ab} + c_2 d^{ab8} \right) \frac{1}{N_c} J^i T^b \\ &+ c_3 \frac{1}{N_c} \{ G^{ia}, N_s \} + c_4 \frac{1}{N_c} \{ J_s^i, T^a \} \\ &+ \frac{1}{3} c_5 \frac{1}{N_c} [J^2, [N_s, G^{ia}]] + \frac{1}{3} (c_1 + c_2) \delta^{a8} J^i, \end{aligned} \quad (35)$$

TABLE 3. Axial couplings.

Fit A	
a_1	1.764 ± 0.042
b_2	-1.218 ± 0.216
d_3	0.549 ± 0.081
c_1	-0.044 ± 0.048
c_2	0.792 ± 0.228
c_3	-0.432 ± 0.036
c_4	0.096 ± 0.072
F	0.39 ± 0.02
D	0.88 ± 0.02
$3F - D$	0.27 ± 0.09

where the coefficients a_1 and b_2 are zeroth order in $SU(3)$ breaking, and the coefficients c_1, \dots, c_5 are first order in the $SU(3)$ breaking. Thus, it is to be understood that the c_i are proportional to ε . Dropping the c_5 operator (since it does not contribute to any of the measured axial couplings) and adding the d_3 operator (to allow the $SU(3)$ parameters D , F and C to have arbitrary values) results in the 7-parameter formula

$$A^{ia} = a_1 G^{ia} + b_2 \frac{1}{N_c} J^i T^a + d_3 \frac{1}{N_c^2} \left(\{J^2, G^{ia}\} - \frac{1}{2} \{J^i, \{J^j, G^{ja}\}\} \right) \quad (36)$$

$$+ \Delta^a \left(c_1 G^{ia} + c_2 \frac{1}{N_c} J^i T^a \right) + c_3 \frac{1}{N_c} \{G^{ia}, N_s\} + c_4 \frac{1}{N_c} \{T^a, J_s^i\} + \frac{1}{\sqrt{3}} \delta^{a8} W^i,$$

where $\Delta_a = 1$ for $a = 4, 5, 6, 7$ and is zero otherwise, and

$$W^i = (c_4 - 2c_1) J_s^i + \frac{1}{N_c} (c_3 - 2c_2) N_s J^i - 3 \frac{1}{N_c} (c_3 + c_4) N_s J_s^i. \quad (37)$$

A comparison of the $1/N_c$ expansion given in Eqs. (36) and (37) with the experimental data was performed in Ref. [28]. The extracted parameters from the experimental fit are tabulated in Table 3¹. As discussed in Ref. [28], c_1 and c_4 are anomalously small, and the character of the fit is not affected in any essential way by neglecting these parameters altogether. The coefficients c_2 and c_3 are suppressed relative to a_1 and b_2 by a factor consistent with a power of $SU(3)$ breaking ε . There is evidence for the $1/N_c$ suppression factors predicted in the $1/N_c$ expansion in the relative magnitudes of coefficients: a_1 and b_2 are comparable, as are c_2 and c_3 , which is what is expected from the $1/N_c$ analysis. However, the fit of Ref. [28] is somewhat unsatisfying in that the χ^2 per d.o.f. is large, which was attributed to probable inconsistency in the experimental data.

A plot in Fig. 8 of the deviations of the baryon axial vector couplings from an $SU(3)$ -symmetric fit is revealing. The $SU(3)$ breaking of the baryon octet axial vector couplings

¹ The parameters used in Eqs. (36) and (37) differ from those in Ref. [28] because $1/N_c$ factors have not been absorbed into the coefficients and because there is an overall factor of 2 difference in the above formula for the axial vector currents compared to the definition in Ref. [28]. The parameters given correspond to Fit A of Ref. [28].

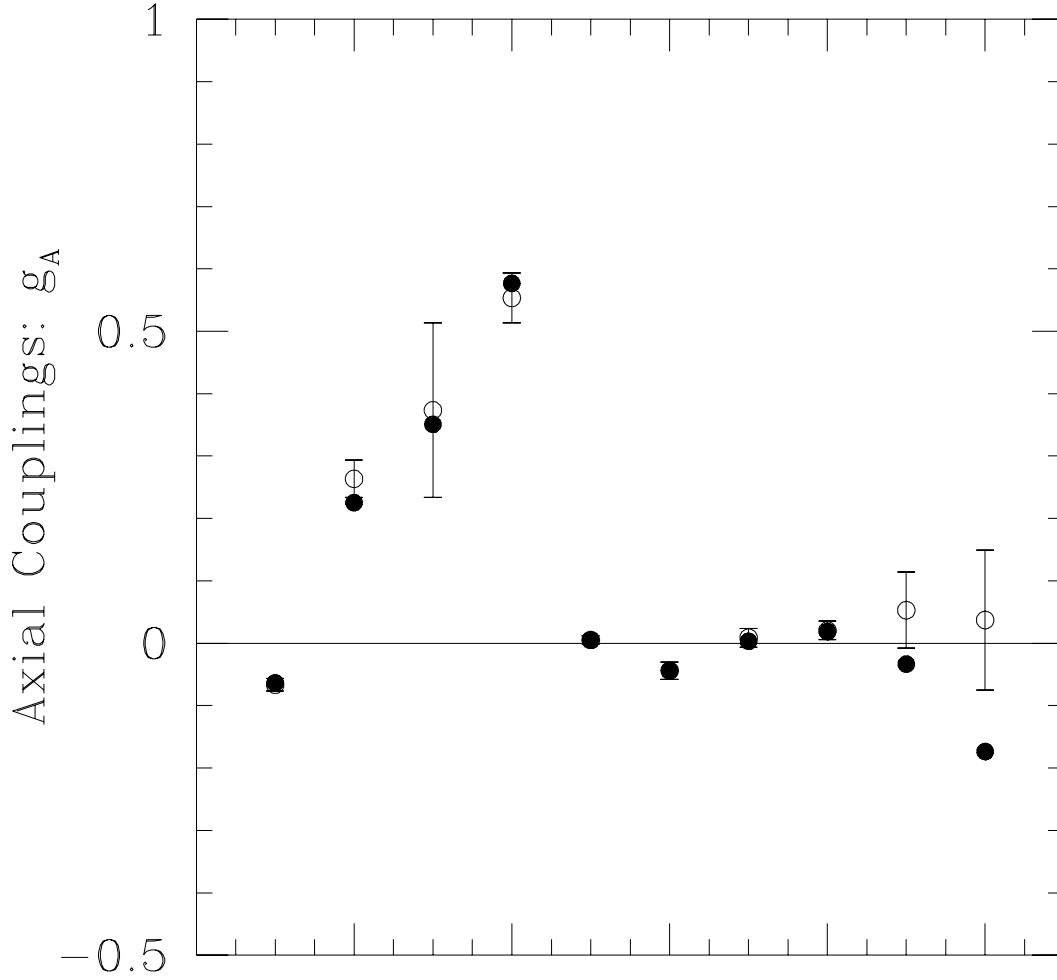


FIGURE 8. Deviation of the axial couplings from the best $SU(3)$ -symmetric fit. The open circles are the experimental data, and the filled circles are the values from Fit A discussed in Ref. [28]. The points plotted are (from left to right) $\Delta \rightarrow N$, $\Sigma^* \rightarrow \Lambda$, $\Sigma^* \rightarrow \Sigma$, $\Xi^* \rightarrow \Xi$, $n \rightarrow p$, $\Sigma \rightarrow \Lambda$, $\Lambda \rightarrow p$, $\Sigma \rightarrow n$, $\Xi \rightarrow \Lambda$, and $\Xi \rightarrow \Sigma$.

obtained from hyperon β -decay measurements is very small, as is well-known. The $1/N_c$ expansion in Eq. (36) predicts the axial vector couplings of the **56** spin-flavor multiplet all together, which means that the $SU(3)$ breaking of hyperon semileptonic decay is related by spin-flavor symmetry to the $SU(3)$ breaking of nonleptonic decay decuplet \rightarrow octet + pion. Thus, the pion axial vector couplings between the decuplet and octet baryons are included with the hyperon β -decay g_{AS} in the fit to $SU(3)$ breaking of the baryon axial vector couplings. Fig. 8 reveals that $SU(3)$ breaking is much larger for the decuplet-octet axial couplings than for the octet-octet couplings, and that an excellent fit is obtained with the exception of the hyperon β decays $\Xi \rightarrow \Lambda$, and $\Xi \rightarrow \Sigma$.

The experimental uncertainty of these two measurements is sizeable, and there are discrepancies between different experimental measurements for these couplings. Thus, it is likely that the experimental data for these decays is not entirely trustworthy, and may account for the large χ^2 per d.o.f. of the fit. Fig. 8 shows that the $1/N_c$ fit favors smaller $SU(3)$ breaking for these couplings.

The first six experimentally measured baryon axial vector couplings in Fig. 8 are isovector couplings, which suggests an analysis using $SU(2) \times U(1)_Y$ flavor symmetry rather than $SU(3)$ flavor symmetry. The $1/N_c$ expansion for baryon isovector axial vector couplings using $SU(2) \times U(1)_Y$ flavor symmetry is given by

$$\begin{aligned}
A^{ia} &= G^{ia} + \frac{1}{N_c} \{N_s, G^{ia}\} \\
&+ \frac{1}{N_c^2} \{N_s, \{N_s, G^{ia}\}\} + \frac{1}{N_c^2} \{J^2, G^{ia}\} + \frac{1}{N_c^2} \{I^2, G^{ia}\} \\
&+ \frac{1}{N_c} J^i I^a + \frac{1}{N_c} J_s^i I^a + \frac{1}{N_c^2} \left\{ J^i, \left\{ G^{ka}, J_s^k \right\} \right\} \\
&+ \frac{1}{N_c^2} \left\{ J_s^i, \left\{ G^{ka}, J_s^k \right\} \right\} + \frac{1}{N_c^2} \{N_s, J^i I^a\} + \frac{1}{N_c^2} \{N_s, J_s^i I^a\}
\end{aligned} \tag{38}$$

where $a = 1, 2, 3$ is an isovector index, and it is to be understood that each operator is multiplied by an unknown coefficient. The matrix elements of G^{ia} for baryons with strangeness of order unity are $O(N_c)$, whereas the matrix elements of J^i , I^a , and J_s^i are $O(1)$, so a valid truncation of the $1/N_c$ expansion is given by

$$A^{ia} = a_1 G^{ia} + a_2 \frac{1}{N_c} \{N_s, G^{ia}\} \tag{39}$$

up to terms which are suppressed by $1/N_c^2$ relative to the leading operator G^{ia} . Eq. (39) yields the equal spacing rule for baryon axial couplings derived in Ref. [12]. The rule implies an equal spacing of the decuplet \rightarrow octet baryon non-leptonic pion couplings which is linear in strangeness,

$$\begin{aligned}
g(\Sigma^* \rightarrow \Sigma\pi) - g(\Delta \rightarrow N\pi) &= g(\Xi^* \rightarrow \Xi\pi) - g(\Sigma^* \rightarrow \Sigma\pi) \\
g(\Sigma^* \rightarrow \Sigma\pi) &= g(\Sigma^* \rightarrow \Lambda\pi).
\end{aligned} \tag{40}$$

This equal spacing rule is clearly evident in the experimental data, as shown in Fig. 8. Eq. (39) also implies $SU(4)$ spin-flavor symmetry for the baryon isovector axial vector couplings in each strangeness sector, so β -decay couplings $n \rightarrow p$ and $\Sigma \rightarrow \Lambda$ are related to the decuplet \rightarrow octet pion couplings with strangeness zero and -1 , respectively. These relations are very well-satisfied.

Magnetic Moments

The magnetic moment operator is $J = 1$ and transforms as the $Q = T^3 + T^8/\sqrt{3}$ component of an $SU(3)$ flavor **8**. The $1/N_c$ expansion of the magnetic moment operator

is the same as for the axial vector couplings with

$$M^i = M^{i3} + \frac{1}{\sqrt{3}} M^{i8} . \quad (41)$$

The isovector magnetic moments are $O(N_c)$ whereas the isoscalar magnetic moments are $O(1)$ at leading order in the $1/N_c$ expansion, so it makes sense to construct $1/N_c$ expansions for the isovector and isoscalar magnetic moments separately[16]. The $1/N_c$ expansion of the isovector magnetic moments is given by

$$M^{i3} = G^{i3} + \frac{1}{N_c} \{N_s, G^{i3}\} , \quad (42)$$

up to terms which are suppressed by $1/N_c^2$ relative to leading 1-body operator G^{i3} . The $1/N_c$ expansion of the isoscalar magnetic moments is given by

$$M^{i8} = J^i + J_s^i + \frac{1}{N_c} \{N_s, J^i\} + \frac{1}{N_c} \{N_s, J_s^i\} , \quad (43)$$

up to terms of order $1/N_c^2$ compared to the two leading order 1-body operators J^i and J_s^i . It is to be understood that every operator in Eqs. (42) and (43) is multiplied by an unknown coefficient of order unity.

There are 21 independent magnetic moments of the baryon octet and decuplet, including transition magnetic moments. These 21 magnetic moments consist of 11 isovector combinations and 10 isoscalar combinations. The $1/N_c$ hierarchy of combinations of isovector and isoscalar magnetic moments is given in Table 4.

The 11 isovector magnetic moment combinations are parametrized in terms of the two operators of Eq. (42), so there are nine isovector magnetic moment relations which are satisfied to order $1/N_c$. These relations are listed as V1 – 9 in Table 4. Only one combination is measured, and the experimental accuracy $10 \pm 2\%$ is consistent with the $1/N_c^2$ prediction of the $1/N_c$ expansion. The $1/N_c$ expansion of the isovector magnetic moments can be truncated to the single operator G^{ia} by eliminating the subleading operator $\{N_s, G^{i3}\}$ operator. The isovector magnetic moment combination corresponding to this subleading operator is $O(1)$ in the $1/N_c$ expansion, or of relative order $1/N_c$ compared to the leading $O(N_c)$ contribution, and is listed as V10₁ in Table 4. The experimental accuracy of this relation is $27 \pm 1\%$, which is consistent with the prediction $1/N_c$ of the $1/N_c$ hierarchy. It is possible to derive a slightly different version of this mass combination by considering an $SU(3)$ analysis. In this analysis, the 2-body operator is $\{T^8, G^{i3}\}$, which is first order in $SU(3)$ breaking and order $1/N_c$ compared to the leading operator. The magnetic moment combination corresponding to this $SU(3)$ operator is listed as V10₂. The experimental accuracy of this relation is $13 \pm 2\%$, which is completely consistent with the theoretic prediction of ϵ/N_c of the $1/N_c$ expansion.

The 10 isoscalar magnetic moment combinations are parametrized by two 1-body operators at leading order in the $1/N_c$ expansion, so there are eight isoscalar magnetic moment relations, which appear as S1 – 8 in Table 4. The $1/N_c$ expansion of Eq. (43) contains four operators, so there are six isoscalar combinations S1 – 6 which are order $1/N_c^2$. The two subleading 2-body operators correspond to isoscalar relations S7 and S8,

TABLE 4. Baryon Magnetic Moments in the $1/N_c$ expansion. The isovector magnetic moments are $O(N_c)$ at leading order, and the isoscalar magnetic moments are $O(1)$. A \checkmark implies that the relation is satisfied to that order in $1/N_c$ to all orders in $SU(3)$ breaking. The experimental accuracies are given for the relations whose magnetic moments have been measured.

	Isovector	$1/N_c$	Flavor	Expt.
V1	$(p-n) - 3(\Xi^0 - \Xi^-) = 2(\Sigma^+ - \Sigma^-)$	$1/N_c$	\checkmark	$10 \pm 2\%$
V2	$\Delta^{++} - \Delta^- = \frac{9}{5}(p-n)$	$1/N_c$	\checkmark	
V3	$\Lambda\Sigma^{*0} = -\sqrt{2}\Lambda\Sigma^0$	$1/N_c$	\checkmark	
V4	$\Sigma^{*+} - \Sigma^{*-} = \frac{3}{2}(\Sigma^+ - \Sigma^-)$	$1/N_c$	\checkmark	
V5	$\Xi^{*0} - \Xi^{*-} = -3(\Xi^0 - \Xi^-)$	$1/N_c$	\checkmark	
V6	$\sqrt{2}(\Sigma\Sigma^{*+} - \Sigma\Sigma^{*-}) = (\Sigma^+ - \Sigma^-)$	$1/N_c$	\checkmark	
V7	$\Xi\Xi^{*0} - \Xi\Xi^{*-} = -2\sqrt{2}(\Xi^0 - \Xi^-)$	$1/N_c$	\checkmark	
V8	$-2\Lambda\Sigma^0 = (\Sigma^+ - \Sigma^-)$	$1/N_c$	\checkmark	$11 \pm 5\%$
V9	$p\Delta^+ + n\Delta^0 = \sqrt{2}(p-n)$	$1/N_c$	\checkmark	$3 \pm 3\%$
V10 ₁	$(\Sigma^+ - \Sigma^-) = (p-n)$	1	\checkmark	$27 \pm 1\%$
V10 ₂	$(\Sigma^+ - \Sigma^-) = \left(1 - \frac{1}{N_c}\right)(p-n)$	1	ϵ	$13 \pm 2\%$
Isoscalar				
S1	$(p+n) - 3(\Xi^0 + \Xi^-) = -3\Lambda + \frac{3}{2}(\Sigma^+ + \Sigma^-) - \frac{4}{3}\Omega^-$	$1/N_c^2$	\checkmark	$4 \pm 5\%$
S2	$\Delta^{++} + \Delta^- = 3(p+n)$	$1/N_c^2$	\checkmark	
S3	$\frac{2}{3}(\Xi^{*0} + \Xi^{*-}) = \Lambda + \frac{3}{2}(\Sigma^+ + \Sigma^-) - (p+n) + (\Xi^0 + \Xi^-)$	$1/N_c^2$	\checkmark	
S4	$\Sigma^{*+} + \Sigma^{*-} = \frac{3}{2}(\Sigma^+ + \Sigma^-) + 3\Lambda$	$1/N_c^2$	\checkmark	
S5	$\frac{3}{\sqrt{2}}(\Sigma\Sigma^{*+} + \Sigma\Sigma^{*-}) = 3(\Sigma^+ + \Sigma^-) - (\Sigma^{*+} + \Sigma^{*-})$	$1/N_c^2$	\checkmark	
S6	$\frac{3}{\sqrt{2}}(\Xi\Xi^{*0} + \Xi\Xi^{*-}) = -3(\Xi^0 + \Xi^-) + (\Xi^{*0} + \Xi^{*-})$	$1/N_c^2$	\checkmark	
S7	$5(p+n) - (\Xi^0 + \Xi^-) = 4(\Sigma^+ + \Sigma^-)$	$1/N_c$	\checkmark	$22 \pm 4\%$
S8	$(p+n) - 3\Lambda = \frac{1}{2}(\Sigma^+ + \Sigma^-) - (\Xi^0 + \Xi^-)$	$1/N_c$	ϵ	$7 \pm 1\%$
Isoscalar/Isovector Relations				
S/V ₁	$(\Sigma^+ + \Sigma^-) - \frac{1}{2}(\Xi^0 + \Xi^-) = \frac{1}{2}(p+n) + 3\left(\frac{1}{N_c} - \frac{2}{N_c^2}\right)(p-n)$	1	ϵ	$10 \pm 3\%$
	$\Delta^{++} = \frac{3}{2}(p+n) + \frac{9}{10}(p-n)$	$1/N_c^2$	\checkmark	$21 \pm 10\%$

which are order $1/N_c$. In addition, S8 is first order in $SU(3)$ breaking. The experimental accuracies of the isoscalar magnetic moment combinations are in complete accord with the $1/N_c$ hierarchy.

Finally, there are two additional relations given in Table 4. S/V_1 is a relation normalizing the isovector magnetic moments to the isoscalar magnetic moments in the $SU(3)$ flavor symmetry limit, and the last relation predicting the Δ^{++} magnetic moment is a linear combination of V2 and S2.

An alternative approach to the magnetic moments is possible using the $1/N_c$ expansion with $SU(3)$ flavor symmetry breaking. The same formula derived for the baryon axial vector currents applies since the magnetic moments also transform as $J = 1$ and as a component of an $SU(3)$ octet in the flavor symmetry limit. The analysis of flavor symmetry breaking involves the same representations analyzed for the baryon axial vec-

TABLE 5. Magnetic moments.

Fit A	
a_1	5.614 ± 0.122
b_2	0.216 ± 0.354
d_3	3.753 ± 0.639
c_1	-1.092 ± 0.230
c_2	0.612 ± 0.276
δc_2	0.066 ± 0.258
c_3	-0.522 ± 0.222
δc_3	0.024 ± 0.312
c_4	0.258 ± 0.228
δc_4	-0.288 ± 0.180

tor couplings, so Eq. (36) can be applied to the magnetic moments. A fit to the baryon magnetic moments using Eq. (36) gives the parameters listed in Table 5 taken from Ref. [28]². For the magnetic moments, the extracted value of b_2 is small, which implies that F/D is very close to the $SU(6)$ symmetry prediction of $2/3$. A plot of the deviations of the baryon magnetic moments from an $SU(3)$ -symmetric fit, given in Fig. 9, shows that $SU(3)$ breaking is considerably larger for the magnetic moments than for the baryon axial vector couplings. Furthermore, $SU(3)$ symmetry breaking for the magnetic moments is dominated by an $O(N_c\sqrt{m_s})$ chiral loop correction, as shown in Fig 10 where the deviation of the baryon magnetic moments from an $SU(3)$ -symmetric fit together with the leading chiral loop correction is plotted. Clearly, the remaining $SU(3)$ breaking in the magnetic moments is much reduced when the leading non-analytic correction is included in the fit. This result also can be seen in Table 5 in terms of the small values of the extracted parameters δc_{2-4} which measure the deviation of the extracted $SU(3)$ breaking parameters c_{2-4} from the flavor symmetry breaking structure given by the dominant chiral loop graph. There is no analogue of this chiral non-analytic correction for the baryon axial vector currents, so the $SU(3)$ breaking patterns of the baryon magnetic moments and the baryon axial vector currents are not similar.

CONCLUSIONS

The $1/N_c$ expansion for QCD baryons is both useful and predictive. In the formal large- N_c limit, there is a spin-flavor symmetry for baryons. For finite N_c , the spin and flavor structure of the baryon $1/N_c$ expansion is prescribed at each order in $1/N_c$. The $1/N_c$ expansion is given in terms of operator products of the generators of the baryon spin-flavor algebra which transform in a certain manner under spin \otimes flavor symmetry. The order in $1/N_c$ of each operator structure is determined in the $1/N_c$ expansion, so the

² Again, the parameters used in Eqs. (36) and (37) differ from those in Ref. [28] because $1/N_c$ factors have not been absorbed into the coefficients and because there is an overall factor of 2 difference in the above formula for the axial vector currents compared to the definition in Ref. [28]. The parameters given correspond to Fit A of Ref. [28].

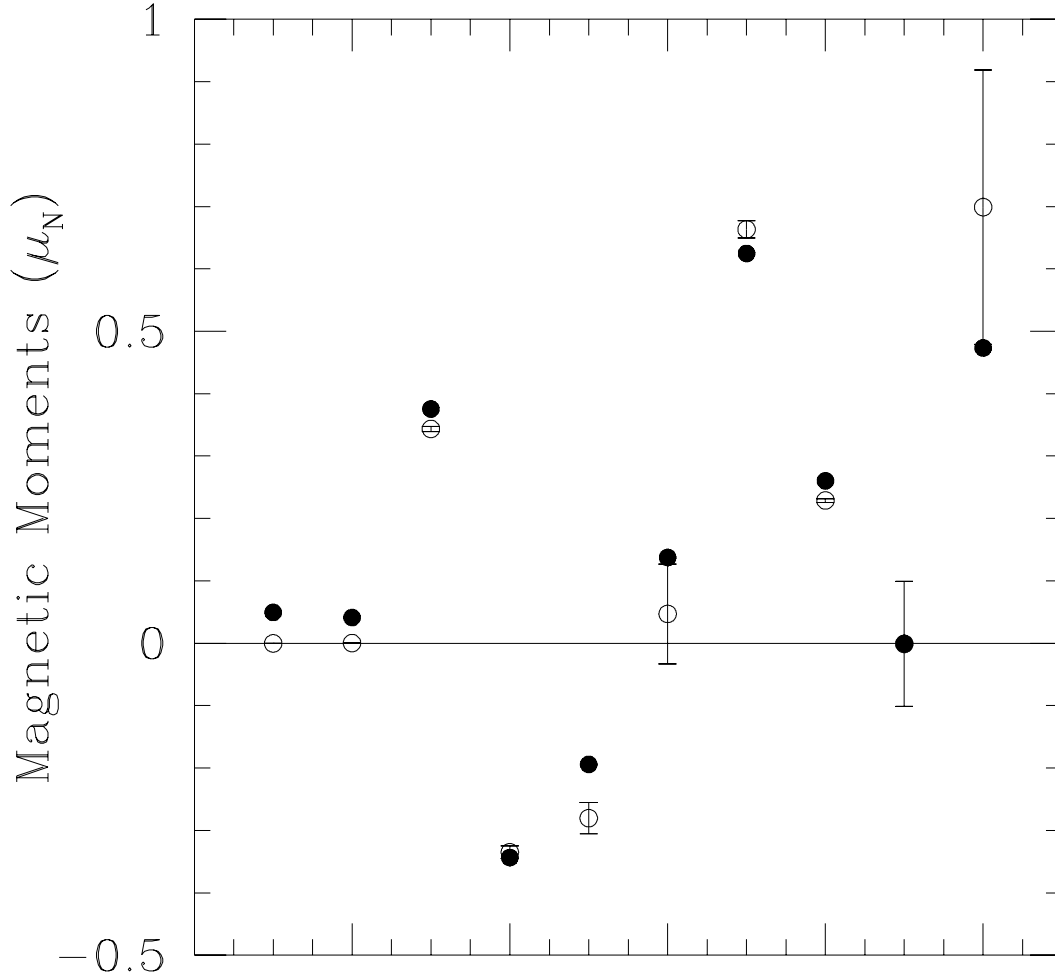


FIGURE 9. Deviation of the magnetic moments from the best $SU(3)$ -symmetric fit. The open circles are the experimental data, and the filled circles are the values from Fit A discussed in the text. The order of the magnetic moments is p , n , Λ , Σ^+ , Σ^- , $\Sigma^0\Lambda$, Ξ^0 , Ξ^- , $p\Delta^+$, and Ω . The Δ^{++} magnetic moment has not been plotted, since the experimental value has a very large error.

$1/N_c$ expansion predicts a hierarchy of spin and flavor relations for baryons in $1/N_c$. The predicted hierarchy of the $1/N_c$ expansion is evident in the baryon masses, axial vector currents and magnetic moments. The pattern of spin-flavor symmetry breaking is quite intricate since $1/N_c$ and $SU(3)$ flavor symmetry breaking are comparable in QCD. The presence of $1/N_c$ suppression factors explains why $SU(3)$ flavor symmetry works to a greater accuracy for baryons than predicted from an analysis of $SU(3)$ breaking alone, and gives a quantitative understanding of spin-flavor symmetry breaking for QCD baryons.

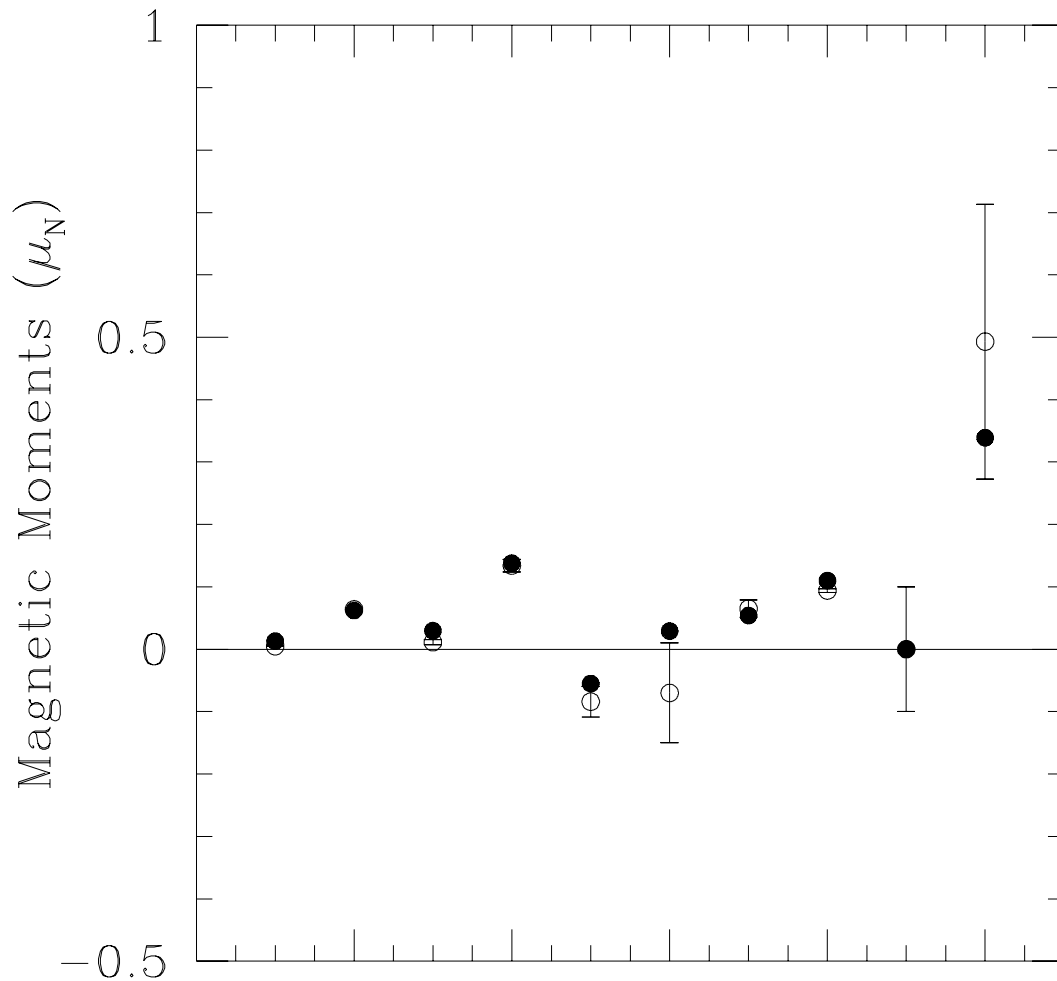


FIGURE 10. Deviation of the magnetic moments from the best $SU(3)$ -symmetric fit plus the leading $O(\sqrt{m_s})$ chiral loop correction. The deviations should be compared with those in Fig. 9.

ACKNOWLEDGMENTS

I wish to thank Jürgen Engelfried and Mariana Kirchbach for organizing such a wonderful workshop. Special thanks to Ruben Flores-Mendieta for his hospitality, and to many of the participants for interesting discussions and experiences. This work was supported in part by the U.S. Department of Energy, under Grant No. DOE-FG03-97ER40546.

REFERENCES

1. Dashen, R., and Manohar, A.V., *Phys. Lett. B* **315**, 425-30 (1993); **315**, 438-40 (1993).
2. Jenkins, E., *Phys. Lett. B* **315**, 431-37 (1993); **315**, 441-46 (1993); **315**, 447-51 (1993).
3. 't Hooft, G., *Nucl. Phys. B* **72**, 461-73 (1974).
4. See Pais, A., *Rev. Mod. Phys.* **38**, 215-55 (1966), and references therein.
5. Manohar, A.V., *Nucl. Phys. B* **248**, 19-28 (1984).
6. Jenkins, E., *Annu. Rev. Nucl. Part. Sci.* **48**, 81-119 (1998).
7. Manohar, A.V., "Large N QCD," in *Les Houches Session LXVIII, Probing the Standard Model of Particle Interactions*, edited by F. David and R. Gupta, Amsterdam, Elsevier, 1998.
8. Veneziano, G., *Nucl. Phys. B* **117**, 519-45 (1976).
9. Witten, E., *Nucl. Phys. B* **160**, 57-115 (1979).
10. Gervais, J-L., and Sakita, B., *Phys. Rev. Lett.* **52**, 87-9 (1984); *Phys. Rev. D* **30**, 1795-1804 (1984).
11. Manohar, A.V., and Jenkins, E., *Phys. Lett. B* **255**, 558-62 (1991); *Phys. Lett. B* **259**, 353-8 (1991).
12. Dashen, R., Jenkins, E., and Manohar, A.V., *Phys. Rev. D* **49**, 4713-38 (1994).
13. Carone, C., Georgi, H., and Osofsky, S., *Phys. Lett. B* **322**, 227-32 (1994).
14. Luty, M., and March-Russell, J., *Nucl. Phys. B* **426**, 71-93 (1994).
15. Carone, C., Georgi, H., Kaplan, L., and Morin, D., *Phys. Rev. D* **50**, 5793-5807 (1994).
16. Jenkins, E., and Manohar, A.V., *Phys. Lett. B* **335**, 452-59 (1994).
17. Dorey, N., Hughes, J., and Mattis, M.P., *Phys. Rev. Lett.* **73**, 1211-14 (1994).
18. Manohar, A.V., *Phys. Lett. B* **336**, 502-7 (1994).
19. Broniowski, W., *Nucl. Phys. A* **580**, 429-44 (1994).
20. Wirzba, A., Kirchbach, M., and Riska, D.O., *J. Phys. G: Nucl. Part. Phys.* **20**, 1583-89 (1994).
21. Takamura, A., et al. *Prog. Theor. Phys.* **93**, 771-80 (1995); Takamura A. *Mod. Phys. Lett. A* **11**, 463-70 (1996).
22. Luty, M., *Phys. Rev. D* **51**, 2322-31 (1995).
23. Luty, M., March-Russell, J., and White, M., *Phys. Rev. D* **51**, 2332-7 (1995).
24. Mattis, M.P., and Silbar, R., *Phys. Rev. D* **51**, 3267-86 (1995).
25. Dashen, R., Jenkins, E., and Manohar, A.V., *Phys. Rev. D* **51**, 3697-3727 (1995).
26. Jenkins, E., and Lebed, R.F., *Phys. Rev. D* **52**, 282-94 (1995).
27. Dorey, N., and Mattis, M.P., *Phys. Rev. D* **52**, 2891-2914 (1995).
28. Dai, J., Dashen, R., Jenkins, E., and Manohar, A.V., *Phys. Rev. D* **53**, 273-82 (1996).
29. Jenkins, E., *Phys. Rev. D* **53**, 2625-44 (1996).
30. Bedaque, P.F., and Luty, M.A., *Phys. Rev. D* **54**, 2317-27 (1996).
31. Jenkins, E., *Phys. Rev. D* **54**, 4515-31 (1996); **55**, 10-12 (1997).
32. Lam, C.S., and Liu, K.F., *Phys. Rev. Lett.* **79**, 597-600 (1997).
33. Kaplan, D.B., and Savage, M.J., *Phys. Lett. B* **365**, 244-251 (1996).
34. Kaplan, D.B., and Manohar, A.V., *Phys. Rev. C* **56**, 76-83 (1997).
35. Goity, J.L., *Phys. Lett. B* **414**, 140 (1997).
36. Pirjol, D., and Yan, T-M., *Phys. Rev. D* **57**, 1449-86 (1998).
37. Pirjol D., and Yan, T-M., *Phys. Rev. D* **57**, 5434-43 (1998).
38. Carlson, C.E., and Carone, C.D., *Phys. Rev. D* **58**, 053005 (1998).
39. Carlson, C.E., Carone, C.D., Goity, J.L., and Lebed, R.F., *Phys. Lett. B* **438**, 327-335 (1998).
40. Carlson, C.E., and Carone, C.D., *Phys. Lett. B* **441**, 363-370 (1998).
41. Carlson, C.E., Carone, C.D., Goity, J.L., and Lebed, R.F., *Phys. Rev. D* **59**, 114008 (1999).
42. Carlson, C.E., and Carone, C.D., *Phys. Lett. B* **484**, 260-266 (2000).
43. Flores-Mendieta, R., Hofmann, C.P., and Jenkins, E., *Phys. Rev. D* **61**, 116014 (2000).
44. Flores-Mendieta, R., Hofmann, C.P., Jenkins, E., and Manohar, A.V., *Phys. Rev. D* **62**, 034001 (2000).
45. Jenkins, E., and Lebed, R.F., *Phys. Rev. D* **62**, 077901 (2000).
46. Jenkins, E., *Nucl. Phys. Proc. Suppl.* **94**, 246-250 (2001).